NASA TECHNICAL NOTE

NASA TN D-7848

NASA TN D-7848

EXPERIMENTAL AND ANALYTICAL SONIC NOZZLE DISCHARGE COEFFICIENTS FOR REYNOLDS NUMBERS UP TO 8×10^6

Andrew J. Szaniszlo

Lewis Research Center
Cleveland, Ohio 44135

NATIONAL AERONAUTICS AND SPACE ADMINISTRATION • WASHINGTON, D. C. • JANUARY 1975

1. Report No. NASA TN D-7848	2. Government Accession No.	3. Recipient's Catalog No.
4. Title and Subtitle EXPERIMENTAL AND ANALYTICAL SONIC NOZZLE DISCHARGE COEFFICIENTS FOR REYNOLDS NUMBERS UP TO 8×10^6		5. Report Date January 1975 6. Performing Organization Code E-8053
7. Author(s) Andrew J. Szaniszlo		8. Performing Organization Report No. 501-24 10. Work Unit No.
9. Performing Organization Name and Address Lewis Research Center National Aeronautics and Space Administration Cleveland, Ohio 44135		11. Contract or Grant No. 13. Type of Report and Period Covered Technical Note
12. Sponsoring Agency Name and Address National Aeronautics and Space Administration Washington, D.C. 20546		14. Sponsoring Agency Code
15. Supplementary Notes		

16. Abstract

Sonic discharge coefficients are obtained for two different geometry flow nozzles using high-pressure nitrogen gas (100 atm) with significant real-gas flow corrections. Throat Reynolds number range extended up to 8×10^6. Discharge coefficients for both nozzles monotonically increase in value at the high throat Reynolds numbers. The 95-percent confidence band for each nozzle is shown. Analytical discharge coefficients for the continuous and finite radius of curvature nozzle are presented. These analytical results for the laminar and turbulent boundary-layer cases are compared to experimental values for sonic flow. Experimental values are also compared to values calculated from the best empirical curve fit equation for subsonic flow.

17. Key Words (Suggested by Author(s))	18. Distribution Statement
Sonic nozzles; Discharge coefficient; Critical flow; Flowmeters; Nozzle geometry	Unclassified - unlimited STAR Category 14

19. Security Classif. (of this report)	20. Security Classif. (of this page)	21. No. of Pages	22. Price*
Unclassified	Unclassified	18	$3.25

* For sale by the National Technical Information Service, Springfield, Virginia 22151

CONTENTS

EXPERIMENTAL AND ANALYTICAL SONIC NOZZLE DISCHARGE COEFFICIENTS FOR REYNOLDS NUMBERS UP TO 8×10^6

by Andrew J. Szaniszlo

Lewis Research Center

SUMMARY

Sonic discharge coefficients are experimentally obtained for two different geometry flow nozzles using high-pressure nitrogen gas (100 atm). One nozzle has a continuous and finite radius of curvature geometry. The other is a long-radius ASME flow nozzle. Each nozzle has a nominal throat diameter of 6.35×10^{-3} meter. Throat Reynolds number range extended up to 8×10^6. Discharge coefficients for both nozzles monotonically increase in value with the high throat Reynolds numbers. Repeatability of the discharge coefficient for each nozzle is shown by a 95-percent confidence band for a single calibration. This bandwidth is less than ±0.2 percent for throat Reynolds numbers greater than 1.6×10^6. Analytically calculated discharge coefficients for the continuous and finite radius of curvature nozzle tested are presented. These analytical results for the laminar and turbulent boundary-layer cases are compared to experimental values. Comparison shows that the real-gas sonic discharge coefficient can be analytically determined to within ±0.2 percent. Experimental values for the long-radius ASME flow nozzle are compared to values calculated from the best empirical curve fit equation for subsonic flow.

INTRODUCTION

The sonic flow nozzle is now being recognized as an accurate, precise, and easy to use head-type of flowmeter for controlling and measuring the mass flow rate of gases over a wide range of flow. References 1 to 4 have pointed out the attractive and distinguishing features that make the sonic flow nozzle practical. Mass flow rate is easy to measure and control since it is directly proportional to upstream pressure level. Upstream pressure tap error is negligible since the approach velocity is small. Absence

of a differential pressure measurement eliminates the throat tap and simplifies construction. Accuracy and ease of use are superior to a subsonic nozzle because the hard to make measurement of the small differential pressure at high pressures like 100 atmospheres is not needed. Downstream pressure pulsations do not affect the mass flow rate because of sonic flow at the throat.

These advantages of a sonic nozzle are now being utilized. Varner (ref. 5) reports using an array of sonic flow venturis as an air metering system in jet engine research. He used discharge coefficient C_D values (i.e., the ratio of the actual mass flow rate to the calculated one-dimensional, isentropic flow rate) analytically determined by Smith and Matz (ref. 6) and real-gas critical flow factors calculated by Johnson (ref. 7). Operating pressure levels in reference 5 were approximately atmospheric. Godt (ref. 8) used sonic flow nozzles as working standards after calibration with a primary device. Nozzle calibration pressure level was less than 22 atmospheres, and the throat Reynolds number was less than 5×10^5. The use of sonic flow nozzles for determining the pressure-level effect on turbine flowmeter performance with natural gas was reported on by Castillon (ref. 9). He relied upon the discharge coefficient equation reported by Vincent (ref. 10) and the natural-gas critical-flow factor of Johnson (ref. 11). Peignelin (ref. 4) extended the work of reference 9 to other flowmeter types. The maximum operating pressure level in references 4 and 9 was about 50 atmospheres. Schroyer (refs. 12 and 13) reports using sonic flow venturis as a secondary standard in natural gas meter development for high pressures and high flow rates. He relied on the simplified analysis of Stratford (ref. 2) for the discharge coefficient values and on the critical-flow factors given by Johnson (ref. 14). None of the previous references have reported experimental C_D data at high-pressure levels where real-gas effects are significant (3 percent) and where the Reynolds numbers are as great as 1×10^7. Such data would demonstrate the accuracy of the technique of combining the analytical C_D values with the critical flow factors given by Johnson (refs. 7, 11, 14, and 15).

There are two main factors that cause the sonic discharge coefficient to be less than unity. First, fluid acceleration near the wall and the resulting inertial forces produce a nonuniform velocity profile (sonic line curvature) at the throat. Vincent (ref. 16) shows that inertial effects can affect the C_D by as much as 1 percent. Secondly, a boundary layer exists along the wall which can lower the C_D by as much as 5 percent at low Reynolds numbers.

Smith and Matz (ref. 6) investigated the inertial and boundary-layer effects in a sonic-flow venturi with a circular-arc convergent section which permitted the value of C_D to be obtained analytically. Their calculation technique gives results that agree with their low pressure (1 to 3 atm) data over a throat Reynolds number range of 7×10^5 to 5×10^6. Stratford (ref. 2) also presents a simplified analysis accounting only for the inertial and boundary-layer effects.

The experimental determination of the sonic C_D variation with throat Reynolds number for two different geometry flow nozzles was the primary purpose of the investigation reported herein. The throat Reynolds number range was 5×10^5 to 8×10^6. The high throat Reynolds numbers were obtained by using nitrogen gas at high-pressure (~100 atm) levels which required real-gas effects to be taken into account. This objective adds new data to the scant amount reported in the literature on sonic flow nozzles and expands the range of sonic C_D values into the regime where real-gas corrections are significant. An additional objective was to analytically calculate the C_D for one of the nozzles and compare the results to the experimental data.

APPARATUS AND TEST PROCEDURE

Nitrogen-Gas Flow Facility

A schematic drawing of the test facility is shown in figure 1. Nitrogen gas supplied from a portable trailer was throttled from 160×10^5 N/m^2 (160 atm) to the desired operating pressure. A bundle of tubes with each tube having a length-diameter ratio of 10 were used just downstream of the pressure regulator to minimize any swirl in the flow. Operating pressure levels varied from 5×10^5 to 100×10^5 N/m^2. Maximum flow rate was 0.75 kilogram per second at the highest pressure level. A sharp-edged orifice (modification of ref. 17) was used as the subsonic flow standard with a maximum differential pressure of 0.48×10^5 N/m^2. The orifice, 60-diameter-length approach pipe, and the 25 diameter-length downstream pipe were calibrated as an integral assembly for the determination of the flow coefficient over the required Reynolds number range. These calibrations were performed with water and air. Inaccuracy of the water stand used for this calibration was less than ±0.2 percent. Differential pressure across the measuring orifice was determined with a fused-quartz Bourdon-tube precision pressure gage (ref. 18). Inaccuracy of this gage is less than ±0.05 percent of full scale. High repeatability of the differential pressure is assured with this gage design by the technique of directly measuring the Bourdon tube deflection optically. The optical detection eliminates errors due to mechanical linkages. Hysteresis errors are practically nonexistent due to the use of fused quartz as the Bourdon tube material. A relatively high-frequency response is obtained due to the Bourdon tube resonant frequency being greater than 20 hertz. The null output from the electro-optical transducer of the gage was displayed on an oscilloscope and time averaged. Lines for the orifice pressure level and differential pressure were separately connected at the orifice taps in a horizontal plane. Differential pressure lines were matched for time constant and time delay by introducing appropriate volumes and sintered porous-metal snubbers in each line. This filter network reduced differential-pressure measurement errors due to absolute pressure-level

fluctuations. These pressure-regulator induced fluctuations had a root-mean-square magnitude of approximately 9 percent of the differential pressure before filtering. The pipe section downstream of the orifice to the nozzle test section as well as the nozzle test section itself were thermally insulated. Insulation helped to give a uniform gas-temperature distribution across the nozzle inlet plane. Gas temperature at the orifice was measured with a thermocouple probe 5.5 pipe diameters downstream of the orifice (ref. 19). Nozzle inlet gas temperature was measured with a thermocouple probe 3.4 pipe diameters upstream of the nozzle inlet. Also, near this location the nozzle upstream static pressure was measured. The static pressure tap error is negligible (ref. 20) since the Mach number equals 0.013. Throat static pressure taps do not exist. Nozzle downstream pressure was measured about 1 pipe diameter downstream of the nozzle exit plane.

A recording potentiometer was used to measure the thermocouple electromotive force from the orifice and nozzle thermocouples with a corresponding temperature inaccuracy of ±0.2 K. The thermocouple reference temperature was the ambient temperature of silicon fluid in a Dewar flask. This temperature was measured to an inaccuracy of ±0.1 K with a thermometer traceable to the National Bureau of Standards (NBS). Operating absolute-pressure-level inaccuracies were no more than ± 0.1 percent. This low inaccuracy level was achieved by using four different sets of gages, of the pressure Bourdon type, to span the pressure range used and by having the gages periodically recalibrated with a dead-weight tester traceable to NBS. Orifice differential pressure inaccuracy was determined to be less than ±0.1 percent. At absolute-pressure levels greater than 30×10^5 N/m^2, the electro-optical transducer output of the gage was corrected by a method described in reference 21.

After instrument calibration and a slow pressurization of the facility to the maximum pressure level for the test to be run, system leak checks and instrument calibrations were performed. Nitrogen gas flow was then initiated by fully opening the throttle valve. The measured upstream to downstream pressure ratio across the test nozzle was always greater than 2 which insured that the flow through the nozzle was indeed sonic. Not until the temperature of the facility had stabilized, approximately 5 minutes later, were data taken. Each data point consisted of a 1-minute run at constant flow rate. The flow rate was then changed by reducing the nozzle upstream pressure with the pressure regulator.

Sonic Nozzle Geometries Selected

Various flow nozzle geometries have been utilized in the past. In particular, those flow nozzles with a circular cylindrical throat section have a high machining reproducibility. Such throat sections combined with a circular quadrant inlet section have a C_D which has been found to be independent of throat Reynolds number changes over a range

of 2×10^5 to 7×10^5 (ref. 3). Also, according to reference 10, the cylindrical throat section has the advantage of minimizing the effect of the convergent section generated nonuniform velocity profile on the sonic C_D. Furthermore, a sufficiently long cylindrical throat would reduce the effect of the convergent section wall profile shape. Therefore, the first flow-nozzle geometry selected (fig. 2) had the traditionally recommended quadrant of an ellipse for the convergent section (ref. 22). This section was tangent to a straight throat section of length 0.6 times the throat diameter. Nozzle inlet-to-throat area ratio was 5.5. The second flow-nozzle geometry was intended to represent the class of wall profiles having a finite, continuous, and constant radius of curvature from the inlet through the throat plane. Such nozzle wall profiles have been examined in references 2, 6, and 16. However, due to machining inaccuracies the radius of curvature of the nozzle utilized (fig. 3) was found to continuously increase in value from the throat plane to the inlet. This wall profile, as with the circular-arc geometry, produces a continuous acceleration of the fluid along the wall to yield a thin boundary layer at the throat. A thin boundary layer combined with this wall profile makes the analytical calculation of the sonic C_D tractable and less inaccurate. An accurate analytical calculation of the C_D provides the sonic flow nozzle with the potential for becoming a compressible flow standard. Additionally, the quadrant sonic nozzle has been reported to be virtually insensitive to back pressure changes when the ratio of the wall radius of curvature to the throat radius (normalized radius of curvature R_N) exceeds unity (refs. 1 and 3). The throat plane R_N for the nozzle fabricated had a value of 2.29. Nozzle inlet- to throat-area ratio was 7. Nozzle throat diameter for both of the nozzles was a nominal 6.35×10^{-3} meter. Throat diameter to upstream pipe diameter ratio β equaled 0.15 for both nozzles. And both nozzles were fabricated from free-machining stainless steel with a specified maximum surface roughness of 8×10^{-7} meter.

RESULTS AND DISCUSSION

In this investigation, as previously mentioned, sonic discharge coefficient values for real-gas conditions were obtained for two different geometry flow nozzles over a throat Reynolds number range of 5×10^5 to 8×10^6. The throat Reynolds number is based upon the plenum viscosity and throat diameter. Experimental data are shown in figures 4 and 5. Also from these tests, nozzle calibration repeatability was determined. Furthermore, experimental C_D data comparison to the analytically calculated values are used to verify the accuracy of the analytical value of the C_D to be used in conjunction with the critical-flow factor (ref. 7).

Accuracy

Repeatability. - A more accurate comparison between the test data and other C_D values is achieved by not only using the mean calibration curve but also from knowing the respective calibration repeatability values. A calibration consists of a set of data points ranging from the maximum to the minimum pressure level of any one of the four pressure-level ranges examined. The resulting individual calibration curve for each pressure-level range will shift from calibration to calibration as indicated by figure 4 which represents the total number of data points from 20 individual calibrations for the long-radius flow nozzle and figure 5 with 21 individual calibrations for the continuous wall-radius nozzle. At a throat Reynolds number greater than 1.6×10^6, the repeatability is ±0.2 percent for a 95-percent confidence band for a single calibration (ref. 23). The confidence band for a single calibration is the band within which it is predicted that all the data points of the next calibration will lie with a 95-percent probability. Stated bandwidths for a single calibration and for the mean are determined from t-distribution statistical calculations using the finite number of data points existing at selected throat Reynolds numbers.

Real-gas factor. - In order to accurately calculate mass flow rate through a sonic nozzle from the high-pressure experimental data, a critical-flow factor is used (ref. 7). This factor corrects the conventional one-dimensional, isentropic flow relation used for calculating the mainstream mass flow rate by accounting for the variation of the ratio of specific heat and the compressibility factor. The value of the critical-flow factor depends upon the pressure and temperature in the nozzle plenum. Neglecting to use this critical-flow factor can give a relative error in mass flow rate exceeding 3 percent at a pressure level of 100×10^5 N/m^2 for nitrogen gas (ref. 24). Such an error can cause the measured C_D to exceed a value of unity.

Any inaccuracy in the critical-flow factor arises from the inaccuracies in the gas property data and in the method of developing the state equation. An approximate value for this uncertainty is obtained by comparing the nitrogen-gas critical-flow factors determined from two different sources of property data (refs. 7 and 15). The comparison shows at a temperature of 275 K and a pressure of 10×10^5 N/m^2 the critical-flow factor from reference 7 exceeds the value from reference 15 by 0.03 percent. Whereas at 100×10^5 N/m^2, the difference is 0.4 percent. This difference increases monotonically with pressure level. The critical-flow factors from reference 7 are used in this report.

Throat area reduction. - Accurate knowledge of nozzle throat area is essential since mass flow rate is directly proportional to it. A relative error in nozzle throat diameter produces twice the relative error in throat area. The throat diameter for both of the test nozzles is a nominal 6.35×10^{-3} meter and is known within ±0.05 percent. Precise determination of the throat diameter for such small flow nozzles demands the highest care in

measurement techniques. Therefore, a correction was made for the fact that the temperature of the nozzle material during calibration is not equal to the temperature during throat diameter measurement. The range of nozzle plenum temperatures for all the tests was 260 to 295 K.

The overall relative inaccuracy associated with the value of C_D is found by combining the relative uncertainties previously stated for each variable. Variables considered are the orifice flow coefficient, orifice and nozzle areas, pressure levels, temperature levels, and the orifice differential pressure. Combining the relative uncertainties for a throat Reynolds number of 1×10^6 (plenum pressure equals 11×10^5 N/m^2) yields an overall root-sum-square relative error of ±0.25 percent (ref. 25). This overall error becomes ±0.44 percent for a throat Reynolds number of 8×10^6 (plenum pressure equals 95×10^5 N/m^2).

Sonic Nozzle Performance

Accurate interpretation of sonic nozzle performance as revealed by the C_D curve shape and its level requires knowledge of the upstream velocity profile. As shown by Ferron (ref. 26), the more uniform the upstream velocity profile the lower the C_D value. Inlet flow to both of the nozzles tested is regarded as fully developed turbulent flow due to the nozzle upstream pipe length to diameter ratio of 60. Also, the measured inlet-temperature profile variation is less than 1 K at the lowest mass flow rate. This essentially uniform temperature profile is due to the thermal insulation placed on the upstream pipe wall.

Initial air calibrations. - Sonic flow nozzle C_D variation with throat Reynolds number at flow conditions where real-gas effects are small was determined for air by using the Lewis flow standards facility. The results are shown in figures 4 and 5. Both of the test nozzles were calibrated with the plenum thermocouple in place. These data provide a reference to which the low throat Reynolds number data from the high-pressure, nitrogen-gas facility can be compared. As seen from figure 4, the agreement between the two facilities is good at the low throat Reynolds numbers.

Long-radius ASME flow nozzle. - A sufficiently high number of data points have been obtained that permits reliable calculation of the sonic nozzle C_D mean curve shape and the 95-percent confidence band for a single calibration and for the mean curve. The mean curve for the sonic C_D variation with throat Reynolds number for this nozzle is shown by figure 4. It ranges in value from 0.988 at a throat Reynolds number of 3×10^5 to 0.992 at a throat Reynolds number of 8×10^6. At the low throat Reynolds number, the level of the C_D curve agrees very well with the independent calibration obtained from the Lewis flow standards facility. This indicates systematic errors from instrumentation

are negligible. Several features are indicated by the variation in the mean C_D curve. First, starting at the low throat Reynolds number, the C_D value increases up to a throat Reynolds number of 1×10^6 which is most probably due to a decreasing boundary-layer thickness. Immediately following is a region of apparent transition from a laminar to a turbulent boundary layer. This region extends over a Reynolds number range of 8×10^5 to 2×10^6. As can be seen from the increased size (±0.3 percent) of the 95-percent confidence band for a single calibration, the C_D value is relatively ill defined over this Reynolds number range.

Any instability is most likely promoted by the local adverse pressure gradient generated by the discontinuous radius of curvature at the juncture of the convergent section with the cylindrical throat section (ref. 27). After this region of apparent transition, the C_D curve monotonically increases in value with throat Reynolds number. At these higher throat Reynolds numbers the 95-percent confidence band for a single calibration is less than ±0.15 percent. Also, the 95-percent confidence band for the mean curve is ±0.05 percent.

A comparison of the sonic nozzle C_D mean curve to the best empirical curve fit equation (ref. 28) for subsonic C_D values is also shown by figure 4. From this comparison, the extent of valid representation, if any, for the sonic C_D mean curve by this empirical equation is obtained. The empirical equation yields the most probable subsonic C_D values for the long-radius ASME flow nozzle. This equation is limited to a maximum throat Reynolds number of 6×10^6 at which the C_D equals 0.993. At throat Reynolds numbers greater than 1.6×10^6 the best empirical curve fit values lie outside the 95-percent confidence band and exceeds the mean curve values for sonic flow by 0.25 percent. Furthermore, the shape of the curve for the subsonic C_D values does not possess any transition region as does the mean curve for sonic-nozzle flow. Finally, the empirical curve fit becomes asymptotic to a constant value of C_D at the high throat Reynolds number whereas the sonic-nozzle C_D mean curve monotonically increases in value. Even though there exists this lack of similarity between the subsonic C_D curve shape and the real-gas sonic C_D mean curve shape, the most probable subsonic C_D values do represent the real-gas C_D values to a practical flowmetering inaccuracy of 1/4 percent.

Continuous wall curvature nozzle. - The mean curve for the sonic C_D variation with throat Reynolds number is shown in figure 5. It ranges in value from 0.989 at a throat Reynolds number of 6×10^5 to 0.991 at a throat Reynolds number of 8×10^6. Coincidentally, this latter C_D value agrees with that of the long-radius flow nozzle. However, the mean curve shapes are quite different. The next feature shown by the shape of the mean curve is the apparent transition for the throat Reynolds number region below 1×10^6. Nevertheless, the exact shape of the mean C_D curve is uncertain at these low throat Reynolds numbers. This uncertainty is indicated by the value of the 95-percent confidence band for the mean curve increasing from ±0.04 percent at a throat Reynolds

number of 1×10^6 to ±0.4 percent at a throat Reynolds number of 6×10^5. For throat Reynolds numbers greater than 1×10^6, the mean C_D curve monotonically increases in value at a greater rate than the long-radius flow nozzle mean curve. Consequently, from the previously mentioned factors for this sonic nozzle geometry, the flow range examined which is free of ill-defined transition regions is noticeably greater than the flow range for the long-radius flow nozzle. At these higher throat Reynolds numbers, the 95-percent confidence band for a single calibration is less than ±0.2 percent.

Comparison to Analytical Results

Nozzle flow model. - Only sonic nozzles with continuous and finite radius of curvature are considered herein. The gas flow through the nozzle is divided into two different flow regions. One is the mainstream gas-flow region that is treated as an irrotational, isentropic flow of a perfect gas. The second is the viscous flow region along the wall occupied by the boundary layer. The effect of each of these two regions on the value of the sonic C_D is separately analyzed. Comparison of the isentropic mass flow rate based upon the inviscid core flow to the one-dimensional mass flow rate gives an inertial discharge coefficient. Final discharge coefficient values are then determined by multiplicatively combining the inertial discharge coefficient with the ratio of effective throat area to the actual throat area determined from the boundary-layer computer program.

The mainstream gas flow parameters across the nozzle throat plane are calculated by using a computer program based upon reference 29 for axisymmetric flow. Calculation results are dependent upon the following input variables: (1) normalized wall radius of curvature at the throat R_N, (2) nozzle throat radius, (3) nozzle axial length, (4) specific heat ratio of the gas, (5) boundary-layer displacement thickness at the throat. The nozzle wall profile, which is not a circular arc, is piecewise curve fitted by the program from reference 30 which enables the determination of the wall Mach number distribution. The inertial discharge coefficient is calculated for a displacement thickness equal to zero. For a nonzero displacement thickness, the final value of the sonic C_D is calculated.

Two-dimensional, boundary-layer parameter values are determined by a computer program from reference 31. The previously mentioned wall Mach number distribution serves as part of the input data to this boundary-layer program. Laminar calculations are based upon the work of Cohen and Roshotko (ref. 32). And the work of Sasman and Cresci (ref. 33) is used as the basis for the turbulent boundary-layer calculations. Modifications to this program with real-gas subprograms of reference 34 permit the accurate calculation of the speed of sound, gas density, and specific heat of nitrogen gas. Furthermore, transport property variation with pressure level is also accounted for by

use of data from references 35, 36, and 37. The resulting boundary-layer displacement thickness at the throat is then used as part of the input to the isentropic gas-core flow program for calculating the final value of the sonic C_D.

Analytical results comparison. - The analytical sonic C_D variation with throat Reynolds number for the continuous wall curvature nozzle is shown in figure 6 for nitrogen gas for both laminar and turbulent boundary-layer conditions. Also shown is the mean sonic C_D curve for the real-gas nitrogen flow data. Agreement between the analytical and experimental curves over the entire throat Reynolds number range experimentally investigated is good considering the previously discussed uncertainty in the mean C_D curve at the low throat Reynolds numbers. However, the analytical C_D variation for the laminar boundary layer differs from the Lewis in-house flow facility calibration by as much as 0.6 percent at the low Reynolds numbers. The difference between the analytical curve for the turbulent boundary layer and the mean C_D curve is equal to or less than 0.2 percent. This difference is within the 95-percent confidence band for a single calibration. A comparison of the level and the slope of the analytical curves to the mean C_D curve tends to verify that the boundary layer is turbulent over the greater extent of the throat Reynolds number range covered. As previously stated, the experimental C_D value is determined by using a real-gas critical flow factor. Considering the previously discussed sources of error, it is seen that the sonic C_D for the nozzle tested can be determined to practical flow metering accuracy by the results from the turbulent boundary-layer calculations including real-gas effects. Therefore, the sonic C_D for any nozzle with a continuous and finite radius of curvature ($R_N > 2$) from the inlet to the throat plane can be expected to be represented over its practical throat Reynolds number range by the previous analytical method for calculating the turbulent boundary layer. This assumes a corner exists at the inlet to augment early transition and thereby extend the useful throat Reynolds number range. The ability to accurately calculate the C_D is highly desirable because it provides the sonic flow nozzle with the potential for becoming a compressible flow standard.

SUMMARY OF RESULTS

The sonic discharge coefficient variation with throat Reynolds number extending up to 8×10^6 was experimentally determined by using high-pressure nitrogen gas with significant real-gas flow corrections. Experimental sonic discharge coefficient values reported on herein have an overall root-sum-square relative error of ±1/4 percent. Two different geometry flow nozzles were studied both having a nominal throat diameter of 6.35×10^{-3} meter. The first flow nozzle was a long-radius ASME design and the second had a continuous and finite radius of curvature. Analytical calculations of the sonic discharge coefficient were done for the latter flow nozzle design with a comparison to the

experimental results. The results of this study are as follows:

1. The sonic discharge coefficient for a nozzle with a continuous and finite radius of curvature and a corner inlet can be determined to within practical flow metering inaccuracy (0.2 percent was obtained in this study) by the analytical means discussed herein.

2. The sonic discharge coefficient for the long-radius ASME nozzle reported on herein can be determined to ±1/4 percent by using the best empirical equation for the most probable subsonic discharge coefficient even though there exists a lack of curve shape similarity.

3. The sonic discharge coefficient values for the nozzles tested do not become asymptotic to a constant value at the high throat Reynolds numbers range examined, but monotonically increase in value up to a Reynolds number of 8×10^6.

4. The sonic discharge coefficient for the continuous wall curvature nozzle tested is free of ill-defined transition regions over a noticeably greater extent of the throat Reynolds number range examined than the long-radius ASME nozzle tested.

5. The sonic discharge coefficient experimental mean curve has a 95-percent confidence band of ±0.05 percent. This value for the mean curve applies to both the long-radius ASME flow nozzle and to the continuous wall curvature nozzle when the Reynolds number exceeds 1×10^6.

Lewis Research Center,
National Aeronautics and Space Administration,
Cleveland, Ohio, September 12, 1974,
501-24.

REFERENCES

1. Arnberg, B. T.: Review of Critical Flowmeters for Gas Flow Measurements. J. Basic Eng., Trans. ASME., vol. 84, Ser. D, no. 4, 1962, pp. 447-460.

2. Stratford, B. S.: The Calculation of the Discharge Coefficient of Profiled Choked Nozzles and the Optimum Profile for Absolute Air Flow Measurements. J. Royal Aero. Soc., vol. 68, no. 640, April 1964, pp. 237-245.

3. Kastner, L. J.; Williams, T. J.; and Sowden, R. A.: Critical-Flow Nozzle Meter and Its Application to the Measurement of Mass Flow Rate in Steady and Pulsating Streams of Gas. J. Mech. Eng. Sci., vol. 6, no. 1, 1964, pp. 88-98.

4. Peignelin, M. G.: Calibration of High Pressure Gas Meters with Sonic Nozzles. J. Instit. Meas. and Control, vol. 5, no. 11, Nov. 1972, pp. 440-446.

5. Varner, C. R.: A Multiple Critical Flow Venturi Airflow Metering System for Gas Turbine Engines. Paper 69-WA/FM-5, ASME, Nov. 1969.

6. Smith, Robert E., Jr.; and Matz, Roy J.: A Theoretical Method of Determining Discharge Coefficients for Venturis Operating at Critical Flow Conditions. J. Basic Eng., Trans. ASME, Ser. D, vol. 84, no. 4, Dec. 1962, pp. 434-446.

7. Johnson, Robert C.: Real-Gas Effects in Critical-Flow-Through Nozzles and Tabulated Thermodynamic Properties. NASA TN D-2565, 1965.

8. Godt, P. W.: Experimental Correlation of Air, Nitrogen, Helium and Argon Flowrates Through Critical Flow Nozzles. Presented at ISA 1st Symposium on Flow - Its Measurement and Control in Science and Industry, Pittsburgh, Pa., May 10-14, 1971.

9. Castillon, M. P.: Calibration of Gas Meters with Sonic Nozzles. Presented at ISA 1st Symposium on Flow - Its Measurement and Control in Science and Industry, Pittsburgh, Pa., May 10-14, 1971.

10. Vincent, Jean: Sur la determination experimentale du coefficient de debit des tuyeres soniques. (Experimental Determination of the Flow Coefficients of Sonic Nozzles.) C. R. Acad. Sci. Paris, t.267, Ser. A, July 1968, pp. 337-340.

11. Johnson, R. C.: Calculations of the Flow of Natural Gas Through Critical-Flow Nozzles. J. Basic Eng., Trans. ASME, vol. 92, no. 3, Sept. 1970, pp. 580-589.

12. Schroyer, Harry R.: Sonic Nozzles for Gas Meter Calibration, Part 1. Pipeline and Gas J., vol. 200, no. 11, Sept. 1973, pp. 31-32.

13. Schroyer, Harry R.: Sonic Nozzles for Gas Meter Calibration, Part 2. Pipeline and Gas J., vol. 22, no. 13, Nov. 1973, pp. 64, 66, 68, 84.

14. Johnson, Robert C.: Real-Gas Effects in the Flow of Methane and Natural Gas Through Critical-Flow Nozzles. NASA TM X-52994, 1971.

15. Johnson, Robert C.: Real-Gas Effects in Critical Flow Through Nozzles and Thermodynamic Properties of Nitrogen and Helium at Pressures to 300×10^5 Newtons per Square Meter (Approx. 300 Atm). NASA SP-3046, 1968.

16. Vincent, Jean: Sur la determination d'un profil optimal de tuyere sonique. (Determination of an Optimum Profile for a Sonic Nozzle.). C. R. Acad. Sci. Paris, t.267, Ser. A, Oct. 1968, pp. 614-616.

17. Standards for Discharge Measurement with Standardized Nozzles and Orifices. German Industrial Standard 1952. Fourth ed., NACA TM 952, 1940.

18. Damrel, J. B.: Quartz Bourdon Gauge. Instrum. Control Systems, vol. 36, Feb. 1963, pp. 87-89.

19. Flow Measurement. Ch. 4 of Power Test Codes Supplements - Instruments and Apparatus. PTC 19.4, ASME, 1959.

20. Rayle, R. E.: Influence of Orifice Geometry on Static Pressure Measurements. Paper 59-A234, ASME, Nov.-Dec. 1959.

21. Szaniszlo, Andrew J.: Pressure Effect on the Sensitivity of Quartz Bourdon Tube Gauges. Rev. Sci. Instrum., vol. 43, no. 5, May 1972, pp. 816-817.

22. Fluid Meters - Their Theory and Application. Sixth ed., ASME, 1971.

23. Dixon, Wilfred J.; and Massey, F. J., Jr.: Introduction to Statistical Analysis. Second ed., McGraw-Hill Book Co., Inc., 1957.

24. Johnson, R. C.: Calculations of Real-Gas Effects in Flow Through Critical-Flow Nozzles. J. Basic Eng., Trans. ASME, vol. 86, no. 3, Sept. 1964, pp. 519-526.

25. Doebelin, Ernest O.: Measurement Systems: Application and Design. McGraw-Hill Book Co., Inc., 1966, pp. 58-64.

26. Ferron, A. G.: Velocity Profile Effects on the Discharge Coefficient of Pressure-Differential Meters. J. Basic Eng., Trans. ASME, Ser. D, vol. 85, Sept. 1963, pp. 338-346.

27. Hall, G. W.: Application of Boundary Layer Theory to Explain Some Nozzle and Venturi Flow Peculiarities. Proc. Inst. Mech. Engrs., vol. 173, no. 36, 1959, pp. 837-870.

28. Benedict, R. P.: Most Probable Discharge Coefficients for ASME Flow Nozzles. Paper 65-WA/FM-1, ASME, Nov. 1965.

29. Kliegel, J. R.; and Quan, V.: Convergent-Divergent Nozzle Flows. AIAA J. vol. 6, no. 9, Sept. 1968, pp. 1728-1734.

30. Smith, Patricia J.: FITLOS: A FORTRAN Program for Fitting Low-Order Polynomial Splines by the Method of Least Squares. NASA TN D-6401, 1971.

31. McNally, William D.: FORTRAN Program for Calculating Compressible Laminar and Turbulent Boundary Layers in Arbitrary Pressure Gradients. NASA TN D-5681, 1970.

32. Cohen, Clarence B.; and Reshotko, Eli: The Compressible Laminar Boundary Layer with Heat Transfer and Arbitrary Pressure Gradient. NACA Rep. 1294, 1956.

33. Sasman, P. K.; and Cresci, R. J.: Compressible Turbulent Boundary Layer with Pressure Gradient and Heat Transfer. AIAA J., vol. 4, no. 1, Jan. 1966, pp. 19-25.

34. Johnson, Robert C.: Calculation of Supersonic Stream Parameters of a Real Gas from Measurable Quantities Using FORTRAN IV Routines. NASA TN D-7653, 1974.

35. Hilsenrath, J., et al.: Tables of Thermodynamic and Transport Properties of Air, Argon, Carbon Dioxide, Carbon Monoxide, Hydrogen, Nitrogen, Oxygen, and Steam. Pergamon Press, 1960.

36. Lenoir, J. M.; and Comings, E. W.: Thermal Conductivity of Gases - Measurement at High Pressure. Chem. Eng. Prog., vol. 47, no. 5, May 1951, pp. 223-231.

37. Lenoir, J. M.; Junk, W. A.; and Comings, E. W.: Measurement and Correlation of Thermal Conductivities of Gases at High Pressure. Chem. Eng. Prog., vol. 49, no. 10, Oct. 1953, pp. 539-542.

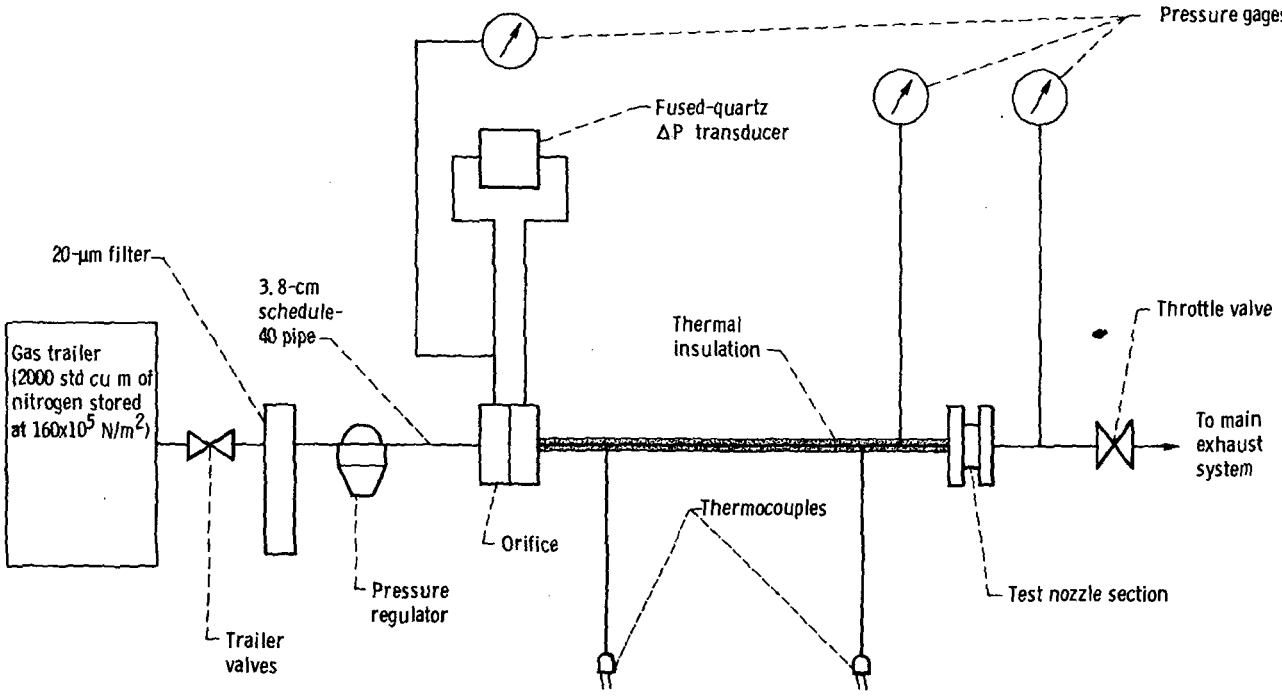

Figure 1. - Nitrogen-gas-flow facility for sonic flow nozzles.

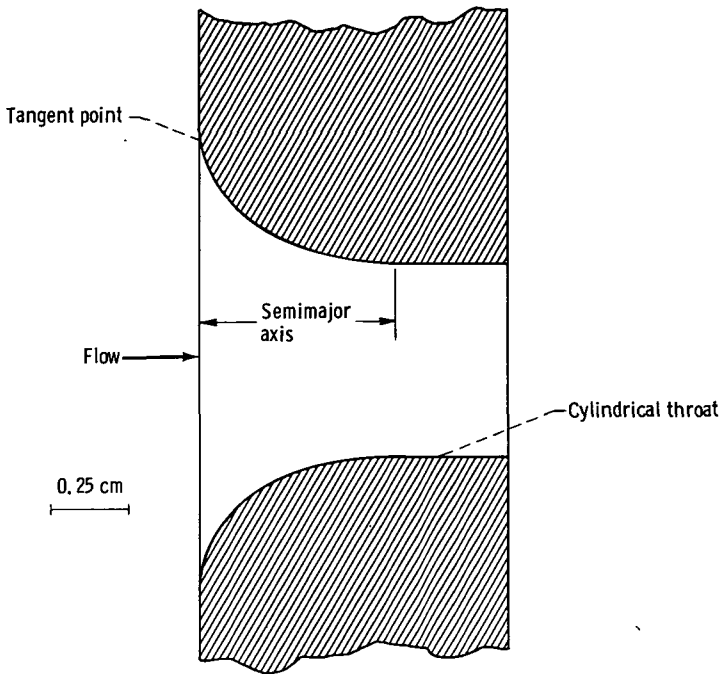

Figure 2. - Long-radius ASME flow nozzle.

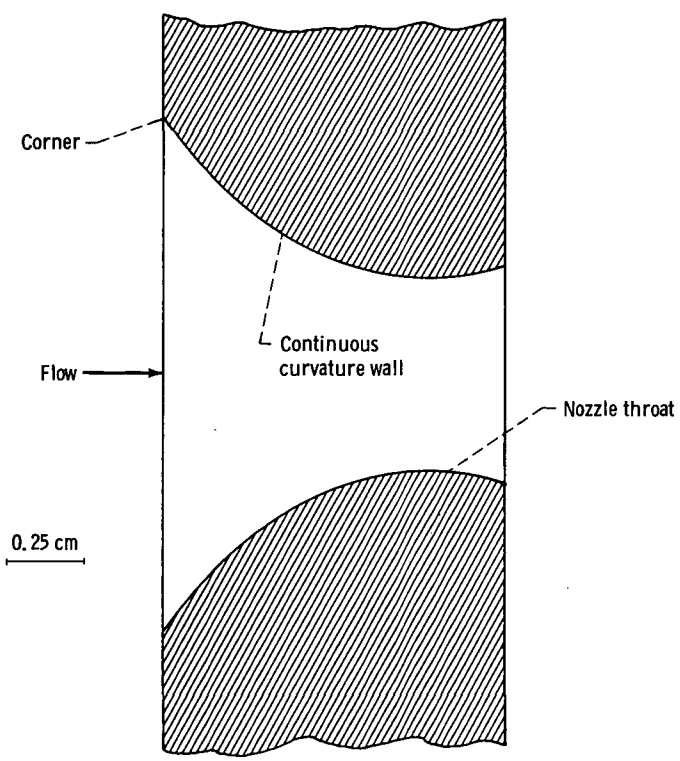

Figure 3. - Continuous wall curvature sonic flow nozzle.

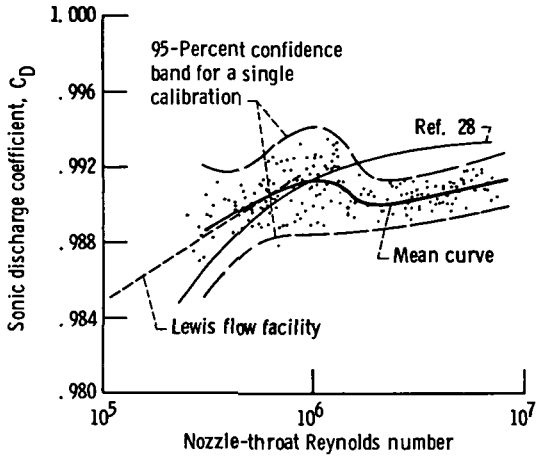

Figure 4. - Experimental discharge coefficients for the long-radius ASME flow nozzle using nitrogen gas.

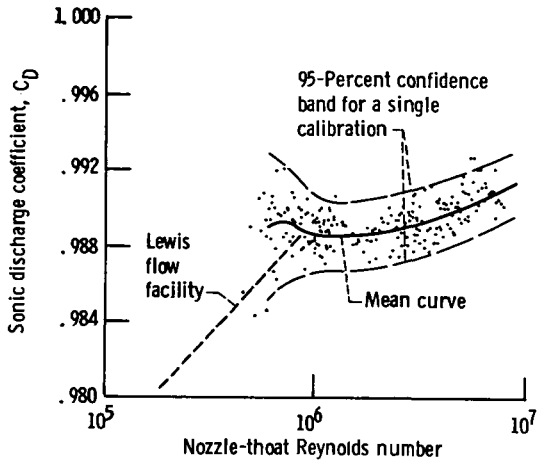

Figure 5. - Experimental discharge coefficients for the continuous wall curvature sonic flow nozzle using nitrogen gas.

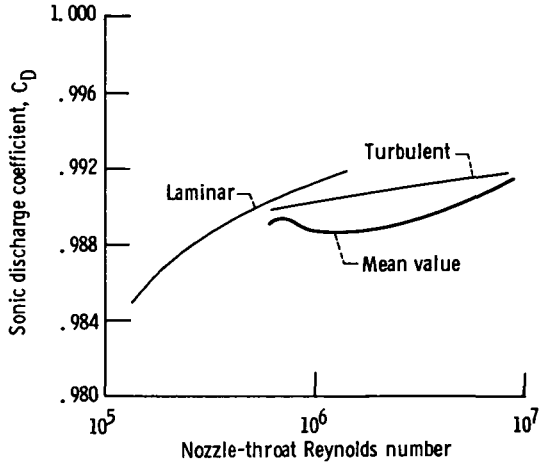

Figure 6. - Comparison of the analytical results to the experimental mean-value curve for the continuous wall curvature sonic flow nozzle.

NATIONAL AERONAUTICS AND SPACE ADMINISTRATION
WASHINGTON, D.C. 20546

OFFICIAL BUSINESS
PENALTY FOR PRIVATE USE $300

SPECIAL FOURTH-CLASS RATE BOOK

POSTAGE AND FEES PAID
NATIONAL AERONAUTICS AND SPACE ADMINISTRATION
451

U.S.MAIL

POSTMASTER : If Undeliverable (Section 158 Postal Manual) Do Not Return

"The aeronautical and space activities of the United States shall be conducted so as to contribute . . . to the expansion of human knowledge of phenomena in the atmosphere and space. The Administration shall provide for the widest practicable and appropriate dissemination of information concerning its activities and the results thereof."

—NATIONAL AERONAUTICS AND SPACE ACT OF 1958

NASA SCIENTIFIC AND TECHNICAL PUBLICATIONS

TECHNICAL REPORTS: Scientific and technical information considered important, complete, and a lasting contribution to existing knowledge.

TECHNICAL NOTES: Information less broad in scope but nevertheless of importance as a contribution to existing knowledge.

TECHNICAL MEMORANDUMS: Information receiving limited distribution because of preliminary data, security classification, or other reasons. Also includes conference proceedings with either limited or unlimited distribution.

CONTRACTOR REPORTS: Scientific and technical information generated under a NASA contract or grant and considered an important contribution to existing knowledge.

TECHNICAL TRANSLATIONS: Information published in a foreign language considered to merit NASA distribution in English.

SPECIAL PUBLICATIONS: Information derived from or of value to NASA activities. Publications include final reports of major projects, monographs, data compilations, handbooks, sourcebooks, and special bibliographies.

TECHNOLOGY UTILIZATION PUBLICATIONS: Information on technology used by NASA that may be of particular interest in commercial and other non-aerospace applications. Publications include Tech Briefs, Technology Utilization Reports and Technology Surveys.

Details on the availability of these publications may be obtained from:

SCIENTIFIC AND TECHNICAL INFORMATION OFFICE

NATIONAL AERONAUTICS AND SPACE ADMINISTRATION

Washington, D.C. 20546